Influence of Water Saturation Time on Microstructure and Mechanical Properties of Jointed Limestone

Huigui Li[1]*, Jun Wang[1,2]*, Xiaohe Wang[2], Wanliang Liang[2], Guosheng Xu[1] and Yingchun Kang[3]

[1]College of Mining Engineering, Guizhou University of Engineering Science, Bijie, China, [2]School of Energy and Mining, China University of Mining and Technology, Beijing, China, [3]China Mining Products Safety Approval and Certification Center, Beijing, China

In order to study the influence of water saturation time on the mechanical properties of jointed limestone, the joint limestone samples with a crack length of 20 mm and a crack angle of 30° are saturated with water for 0, 1, 3, 5 and 7 days and tested with the RMT-150C mechanical test machine. The results show that the water saturation time has a significant effect on the stress-strain curve, peak strength, elastic modulus, crack development and failure characteristics of the jointed limestone. There is a step rise or fall phenomenon near the peak stress. The peak strength and elastic modulus of the joint limestone are significantly negatively correlated with the saturated time. Compared with that of the saturated 0-day sample, the peak compressive strength of the saturated 1-day, 3-day, 5-day and 7-day samples was decreased by 16.5%, 24.7%, 43.6%, and 47.7%, respectively, and the elastic modulus decreased by 11.0%, 32.0%, 45.0%, and 67.9%, respectively. Saturated water cracks the skeleton particles of the limestone samples, and the length of the microscopic pores and fissures increased gradually. The phenomenon that the number and length of cracks increase with the increase of the water saturation time will weaken the mechanical properties of the jointed limestone. The physical and chemical reactions, lubrication, and pore water pressure produced by water-saturated water-rock interactions make it easier for the Mohr stress circle to reach the limit equilibrium state. Saturated water reduces the degree of fragmentation of the sample, and the integrity of the fracture surface is higher after failure. The findings in this paper are helpful to further reveal the mechanism of the crushing of supports and the frequent occurrence of water gushing accidents at the working face in the Xinhua region of northwestern Guizhou.

Keywords: water saturation time, jointed limestone, mechanical properties, uniaxial compression, microstructure

INTRODUCTION

There are many discontinuities such as joints, fissures and interlayers in the rock mass, which will greatly weaken the stability of the rock mass. For the rock mass in the roof of the coal seam, in addition to a large number of discontinuous surfaces, there is often a large amount of water in the discontinuous surfaces. The presence of water will promote the further development of the discontinuity, resulting in the fracture of the rock mass. In particular, due to the long-term action of water, the physical and mechanical properties of the rock in the aquifer will change, which has a great impact on the stability of the overlying rock and the surrounding rock of the

roadway (Deng et al., 2017a; Duan and Ren, 2019; Wang et al., 2019). The mechanical model has played an important role in the study of jointed rock formation and rock mechanics. Many scientists have carried out related research on the mechanical model of jointed rock. Zhao et al. (2020) used the discrete element software 3DEC to establish a numerical model to analyze the mechanical and failure characteristics of jointed rocks under uniaxial tension. Meng et al. (2019) proposed a modeling method based on homogenization to study the influence of columnar joint structure on the mechanical properties of rock mass. Yang et al. (2019) used the theory of damage mechanics to explore multiple groups of joints distributed in the rock mass, and established a damage mechanics model. Liu et al. (2016) studied non-penetrating jointed rock mass and developed a dynamic damage constitutive model under uniaxial compression. Li H. G. et al., (2020), Li et al. (2021), Li et al. (2020b) use siltstone, medium grained sandstone, coarse-grained sandstone and coal in the strata of Bulianta coal mine and Buertai coal mine in Shendong mining area as the research object, and analyzed the influence of interlayer thickness on the mechanical properties of jointed rock. They found that the thickness of the interlayer has a significant effect on the mechanical properties of the jointed coal rock and the interlayer thickness has a significant influence on the mechanical properties of the jointed coal rock. Li et al. (2019), Fan et al. (2020), Li (2020a), Li (2022) used finite element simulation and structural mechanics to investigate the positive correlation effect of fracture occurrence state on rock failure degree, and the influence of structural joints, etc. on the occurrence state of shale gas. 3D printing technology is increasingly applied to the study of jointed rock mass. Huang et al. (2020) combined Voronoi diagram stochastic simulation and 3D printing technology to prepare an irregular columnar joint network model and analyze the mechanical properties of irregular columnar joint rock mass. The results show that the columnar joints have a significant effect on the uniaxial compressive strength. Xia et al. (2020) used 3D printing technology to produce three-dimensional irregular columnar jointed rock mass, and analyzed the influence of irregular columnar joints on the mechanical behavior of jointed rock mass.

To study the physical and mechanical properties of water-saturated rocks, Vasarhelyi (2005) examined the negative correlation between water content and limestone strength by using statistical methods. Yilmaz (2010) studied the deterioration effect of water content on gypsum strength and deformation. Niu et al. (2018) analyzed the mechanical characteristics and energy evolution mechanism of water-saturated sandstone through post-peak cyclic loading and unloading tests on coarse sandstone samples, and found that water saturation reduced the total absorbed energy, dissipated energy and elastic strain of rock samples. Su et al. (2017) carried out uniaxial tests on the natural water-filled roof sandstone of coal seams. The results showed that the strength and deformation parameters of the sandstone samples are weakened by saturated water to varying degrees. Li et al. (2018) conducted a study on the influence of water saturation time on the deterioration of physical and mechanical properties of slate, and quantitatively evaluated the degree of damage and deterioration of slate from a macroscopic

perspective through mass and strength variables. Zhang et al. (2019) took argillaceous siltstone as the research object, and obtained the damage and deterioration laws of argillaceous siltstone affected by water content, such as strength, deformation characteristics and failure mode. Wang et al. (2016), Wang et al. (2017), Wen et al. (2017), and Zheng et al. (2017) studied the mechanical parameters of coal and sandstone in their saturated state by using the combined dynamic and static loading method. They found that the saturated state had a significant effect on the dynamic mechanical parameters of coal and sandstone. Yang et al. (2018) adopted a similar simulation method, conducted a similar single-fissure rock mass freezing triaxial test, and concluded that the mechanism of increasing rock mass strength with decreasing temperature led to an increase of the freezing of rock mass pore water and fissure water into ice. Moreover, the inclination angle of the fracture affected the initial position of the fracture surface, the trace length affected the expansion scale of the fracture surface, and the confining pressure affected the extension direction of the fracture surface. It was concluded that the dip angle had the greatest influence on the strength of the rock mass, followed by the trace length, and the temperature had the least influence. Deng et al. (2017b) reported that the influence of water content on the tensile strength of layered sandstone was the deterioration of macroscopic mechanical properties caused by the change in microstructure. Li B. et al. (2020) analyzed the unloading confining pressure characteristics of shale with different water contents, and believed that the deformation parameters and strength parameters of shale were significantly affected by water. When the shale is saturated with water, the inter-particle cementation is loose, which improves the crack propagation ability and reduces the weakening of its macro-mechanical properties such as strength and deformation. Li J. et al. (2020) took the weathered granite from Mount Tianshan in Xinjiang as the research object, analyzed the strength and deformation characteristics of water-saturated weathered granite at different temperatures and different confining pressures, and pointed out that when the temperature decreased, the saturated water further increased the friction and improved the rock strength.

In summary, researchers have conducted a number of studies on the influence of joints and fissures on the physical and mechanical properties of rocks, and have also carried out related research on sandstone, argillaceous siltstone, granite, slate, etc. Systematic laws have been revealed in the influence of water on the physical and mechanical characteristics of sandstone and the influence of joints and fissures on the physical and mechanical properties of rock. However, there is little research on the changing laws of physical and mechanical properties of rocks in their water saturated state. There are a large number of aquifers with joints and fissures in the overlying strata of the coal seam. Therefore, it is particularly important to study the influence of saturated water on the physical and mechanical properties of the jointed strata. Since April 2016, there have been 22 water gushing accidents at the working face caused by the mining of the M9 coal seam in Xinhua District. One of the main reasons for the accidents was the limestone fault of the Changxing

FIGURE 1 | Dry rock samples.

limestone was cored, cut and ground to make standard samples with Φ×H of 50 mm × 100 mm sample. After the samples were made, a 4 mm circular hole was drilled in the center of each sample, and then a crack with a length of 20 mm, a width of 2 mm, and an angle of 30° angle to the bottom was cut by hydraulic slitting. The joint angle is consistent with that observed on site. The samples are divided into 5 groups. The samples in Group A are dry samples, and the sample numbers are A1 to A3. The samples in Group B, Group C, Group D and Group E are soaked samples, soaked for 1 day, 3 days, 5 days, respectively. They are numbered B1-B3, C1-C3, D1-D3 and E1-E3, respectively. There are 3 samples in each group. The group of dry samples prepared is shown in **Figure 1**, and the parameters of all groups of samples are listed in **Table 1**.

Sample Preparation

The mechanical experiment was carried out by using the RMT-150C mechanical test system designed by Wuhan Institute of Geomechanics, China. In this experiment, the displacement controlled loading method is adopted. The loading rate during the experiment was 0.002 mm/s. The experiment was repeated 3 times for each group of samples.

Formation overlying the M9 coal seam. The limestone of the Changxing Formation is an aquifer and is the main source of water for the water influx accidents at the working face. Water has a great impact on the physical and mechanical properties of the limestone in this group, and also has a great influence on the breaking form of the overlying rock at the working face, especially after the rainy season. Therefore, it is urgent to study the physical and mechanical properties of the Changxing Formation limestone in this area under different water-saturated states. In this paper, with the limestone from the limestone fault in the Changxing Formation in northwestern Guizhou as the research object, the relationship between the uniaxial compressive strength, elastic modulus and other parameters of the jointed limestone and the water saturation time is studied.

SAMPLE PREPARATION AND EXPERIMENTAL SCHEME

Sample Preparation

The limestone samples were collected from the Xinhua region in northwest Guizhou, and transported to the university laboratory. According to the requirements of the specification Ministry of Coal Industry of the Peoples Republic of China, (1988), the

INFLUENCE OF WATER SATURATION TIME ON MECHANICAL PROPERTIES OF JOINTED LIMESTONE

Characteristic Analysis of Stress-Strain Curve

To study the influence of water saturation time on the mechanical properties of jointed limestone, uniaxial compression tests were carried out on the jointed limestone samples saturated with water for 0, 1, 3, 5, and 7 days by using the RMT-150C mechanical testing machine. **Table 2** shows the mechanical parameters of the jointed limestone with different water saturation times under uniaxial compression. **Figures 2A–E** are the stress-strain relationship curves of the jointed limestone with different

TABLE 1 | Basic parameters of jointed limestone samples.

Sample No.	Crack angle/°	Crack length/mm	Height/mm	Diameter/mm	Saturation time/day
A1	30	20	100.70	49.76	0
A2	30	20	100.84	49.47	0
A3	30	20	99.98	49.53	0
B1	30	20	97.68	49.47	1
B2	30	20	100.73	49.49	1
B3	30	20	101.07	49.50	1
C1	30	20	99.93	49.54	3
C2	30	20	100.77	49.46	3
C3	30	20	100.55	49.51	3
D1	30	20	99.73	49.55	5
D2	30	20	100.90	49.41	5
D3	30	20	100.10	49.59	5
E1	30	20	100.41	49.52	7
E2	30	20	101.24	49.49	7
E3	30	20	100.68	49.48	7

TABLE 2 | Mechanical parameters of jointed limestone with different water saturation time under uniaxial compression.

No.	Crack angle/°	Crack length/mm	Saturation time/day	σ_c/MPa	σ_p/MPa	E/GPa	E_p/GPa	Notes
A1	30	20	0	71.06		42.10		
A2	30	20	0	70.13	72.77	41.14	45.15	
A3	30	20	0	77.11		52.21		
B1	30	20	1	68.87		32.03		
B2	30	20	1	58.25	60.74	45.51	40.20	
B3	30	20	1	55.10		43.07		
C1	30	20	3	58.25		34.47		
C2	30	20	3	56.24	54.82	29.69	30.72	
C3	30	20	3	49.97		28.00		
D1	30	20	5	40.32		23.45		
D2	30	20	5	42.36	41.01	23.42	24.84	
D3	30	20	5	40.36		27.65		
E1	30	20	7	37.08		14.02		
E2	30	20	7	—	38.07		14.51	Failure
E3	30	20	7	39.06		14.99		

water saturation times under uniaxial compression. The stress-strain curve of the uniaxial compression of the E2 specimen is missing in **Figure 2E**. During the experiment, the power supply of the computer was suddenly cut off, so that this group of data was not recorded. However, since the samples in this experiment were all collected from the same location, there were no remaining samples, so no supplements were made. experiment. **Figures 2A, E** indicate that the water saturation time has a significant effect on the stress-strain curve of the jointed limestone. When the water saturation time is 0, 1, 3, 5, and 7 days, the stress-strain curve basically presents three stages, namely: initial compaction stage, linear elastic stage, and plastic deformation failure stage. None of the samples have residual strength. They all break suddenly after the peak stress, because limestone is a relatively brittle rock. However, with the increase of the water saturation time, the characteristics of the stress-strain curve show a difference. The strain in the initial compaction period is larger, the curve becomes gentler, the slope of the curve in the linear elastic stage gradually decreases, and there is a step-up phenomenon in the peak stress stage.

Analysis of Influence of Water Saturation Time on the Strength of Jointed Limestone

Table 2 shows the mechanical parameters of the jointed limestone with different water saturation times under uniaxial compression, where σ_c is the uniaxial compressive strength, E is the elastic modulus, σ_p and Ep are the average uniaxial compressive strength and the average elastic modulus, respectively. With **Table 2** and **Figure 3** combined, it can be found that the saturation time has a significant effect on the peak compressive strength of the jointed limestone. The uniaxial compressive strengths of the jointed limestone at water saturation times of 0, 1, 3, 5, and 7 days are 72.77, 60.74, 54.82, 41.01 and 38.07 MPa, respectively, which are lower than that with no water saturation by 16.5%, 24.7%, 43.6%, and 47.7%, respectively. These data indicated that there is an obvious
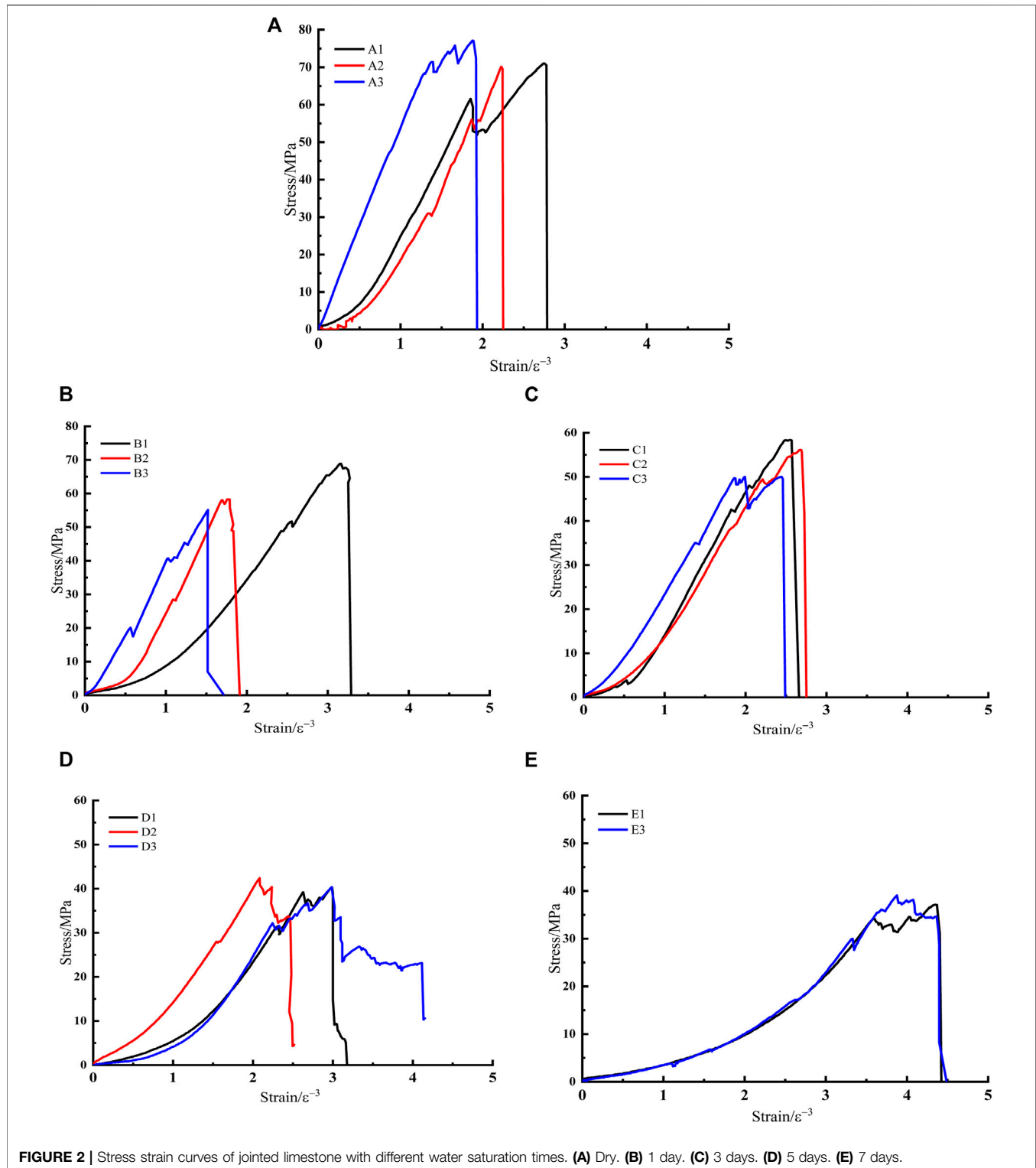
negative correlation between the uniaxial compressive strength of the sample and the saturated time. Comparison of the strength of the saturated sample for 1 day and the dry sample shows that water has a significant effect on the strength of limestone. The uniaxial compressive strength of limestone decreases greatly when the water saturation time is 3–5 days, and the negative correlation effect of water content on limestone is obviously slowed down after saturated for 5 days, which shows that when the joints are saturated for about 5 days in the natural state, the moisture content of limestone reaches relative saturation. **Figure 3** shows the relationship between the peak compressive strength of the jointed limestone and the water saturation time. With the above analysis and **Figure 3** combined, it can be found that the peak compressive strength of the jointed limestone has a negative correlation with the water saturation time. With the increase of the water saturation time the peak compressive strength decreases gradually. The relationship is fitted by curve fitting. The fitting equation is shown in **Eq. 1**, and the correlation coefficient is 0.94, which indicates that the correlation is good.

$$\sigma_c = 71.32 - 7.86t + 0.43t^2 \tag{1}$$

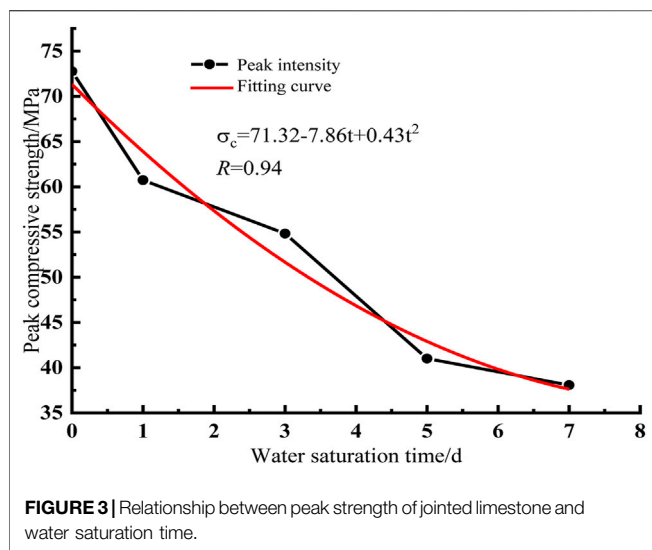where σ_c is the peak compressive strength, MPa; t is the water saturation time, d.

Analysis of influence of water saturation time on elastic modulus of jointed limestone.

To investigate the influence of water saturation time on the elastic modulus of the jointed limestone, the relationship between the elastic modulus of the jointed limestone and the saturation time was analysed. **Figure 4** shows the relationship between the elastic modulus and the saturation time. It can be seen from **Table 2** and **Figure 4** that when the jointed limestone is saturated with water for 0 day, 1 day, 3, 5, and 7 days, the variation range of the elastic modulus is 41.14 ~ 52.21 GPa, 32.03 ~ 45.51 GPa, 28.00 ~ 34.47 GPa, 23.42 ~ 27.65 GPa, 14.02 ~ 14.99 GPa, and the average elastic modulus is 45.15, 40.20, 30.72, 24.84, 14.51 GPa,

FIGURE 2 | Stress strain curves of jointed limestone with different water saturation times. **(A)** Dry. **(B)** 1 day. **(C)** 3 days. **(D)** 5 days. **(E)** 7 days.

respectively. These data indicated that the saturated time not only has a significant impact on the peak compressive strength of the jointed limestone, but also has a significant impact on the elastic modulus of the jointed limestone. Furthermore, the elastic modulus of the jointed limestone is also negatively correlated

with the saturation time. Compared with that for 0 day, the elastic modulus of the jointed limestone saturated with water for 1 day, 3, 5 and 7 days is decreased by 4.95, 14.43, 20.31, and 30.64 GPa, with a decrease rate of 11.0% and 32.0 %, 45.0%, 67.9%, respectively. Through the above analysis, the relationship is

FIGURE 3 | Relationship between peak strength of jointed limestone and water saturation time.

FIGURE 4 | Relationship between elastic modulus of jointed limestone and water saturation time.

fitted by linear fitting, the fitting equation is shown in **Eq. 2**, and the correlation coefficient is 0.99, which indicates that the correlation is good.
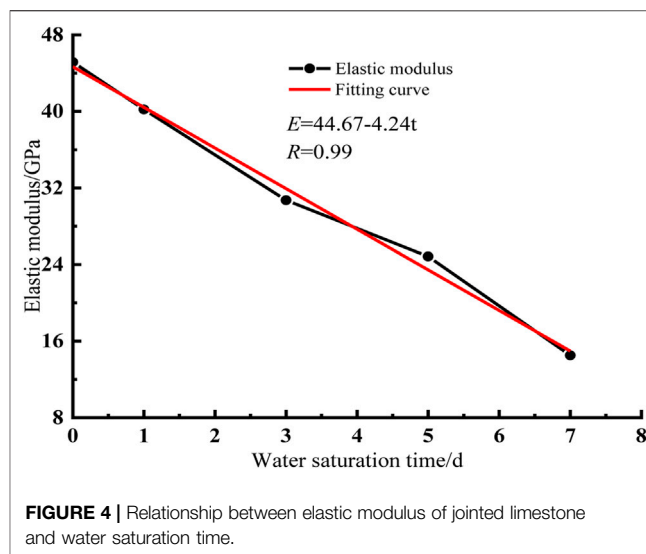
$$E = 44.67 - 4.24t \qquad (2)$$

where E is the elastic modulus of the jointed limestone, GPa; t is the saturation time, d.

EFFECT OF WATER SATURATION TIME ON MICROSTRUCTURE OF JOINTED LIMESTONE

To study the effect of water saturation time on the microstructure of the jointed limestone, the microstructure of the limestone samples dried, saturated with water for 1, 3, 5 and 7 days was observed on an environmental scanning electron microscope (FEI-SEM) in the Institute of Geochemistry, Chinese Academy of Sciences. The limestone samples were magnified 5000 times and 10,000 times, respectively. Moreover, to study the influence of water saturation time on the length and width of pores and fissures and the number of pores and fissures in the microstructure of limestone, the professional processing software Smileview was used to measure the length and width of microcracks of five limestone samples with different water saturation times, as shown in **Figure 5**. **Figure 5** indicates that the number of micropores and cracks in the dried sample is very small, and the cracks mainly exist between the particles. However, with the increase of the water saturation time, the number of micropores and fractures in the limestone samples gradually increases, and fractures began to appear in the grains, resulting in the fracture of the skeleton grains. **Figure 5** shows that a large number of microscopic cracks appear in the limestone sample saturated with water for 7 days, mainly in the interior of the particles. The length of microcracks in the limestone samples increases significantly with the increase of the water saturation time.

Table 3 is a statistical table of the lengths and widths of microscopic pores and fissures of the limestone samples dried and saturated with water for 1, 3, 5 and 7 days. There are differences in the lengths and widths of microscopic pores and fissures of the samples, and the water saturation time has a significant effect on the length and width of the microscopic pores and fissures of the limestone samples, especially the length of the microscopic pores and fissures of the limestone samples. The length gradually increases with the increase of the water saturation time. The length ranges of the microscopic pores and fissures of the limestone samples dried and saturated with water for 1, 3, 5 and 7 days are 0.11 ~ 5.57 μm, 0.50 ~ 5.98 μm, 0.60 ~ 7.97 μm, 0.70 ~ 8.20 μm and 1.11 ~ 9.32 μm, respectively. This indicates that with the gradual increase of the water saturation time, the minimum and maximum lengths of the microscopic pores and fissures in limestone gradually increase, showing a positive correlation. The average lengths of the microscopic pores and fissures of the limestone samples dried and saturated with water for 1, 3, 5 and 7 days are 1.62, 2.05, 2.52, 2.79 and 4.23 μm, respectively. Compared with that of the dried samples, the micro-crack lengths of the samples saturated with water for 1, 3, 5 and 7 days are increased by 26.5%, 55.6%, 72.2%, and 161.1%, respectively. Furthermore, with the increase of the saturation time, the number of cracks increases significantly, and most of the cracks appear in the middle of the particles, which is one of the main reasons for the change of macroscopic mechanical parameters. In addition, the width ranges of the microscopic pores and fissures of the limestone samples dried and saturated with water for 1, 3, 5 and 7 days are 0.08 ~ 0.80 μm, 0.10 ~ 1.32 μm, 0.14 ~ 1.65 μm, 0.17 ~ 0.97 μm and 0.25 ~ 2.55 μm, respectively, and the average values of the microscopic pore and fissure widths are 0.45, 0.41, 0.40, 0.74 μm, respectively. The minimum value of the pore and fissure width increases gradually with the increase of the water saturation time, and the maximum value also fluctuates.

Figure 6 shows the characteristic diagram of the microscopic pore and fracture parameters of the limestone samples dried and saturated with water for 1 day, 3, 5 and 7 days. As indicated in **Figure 6**, there are significant
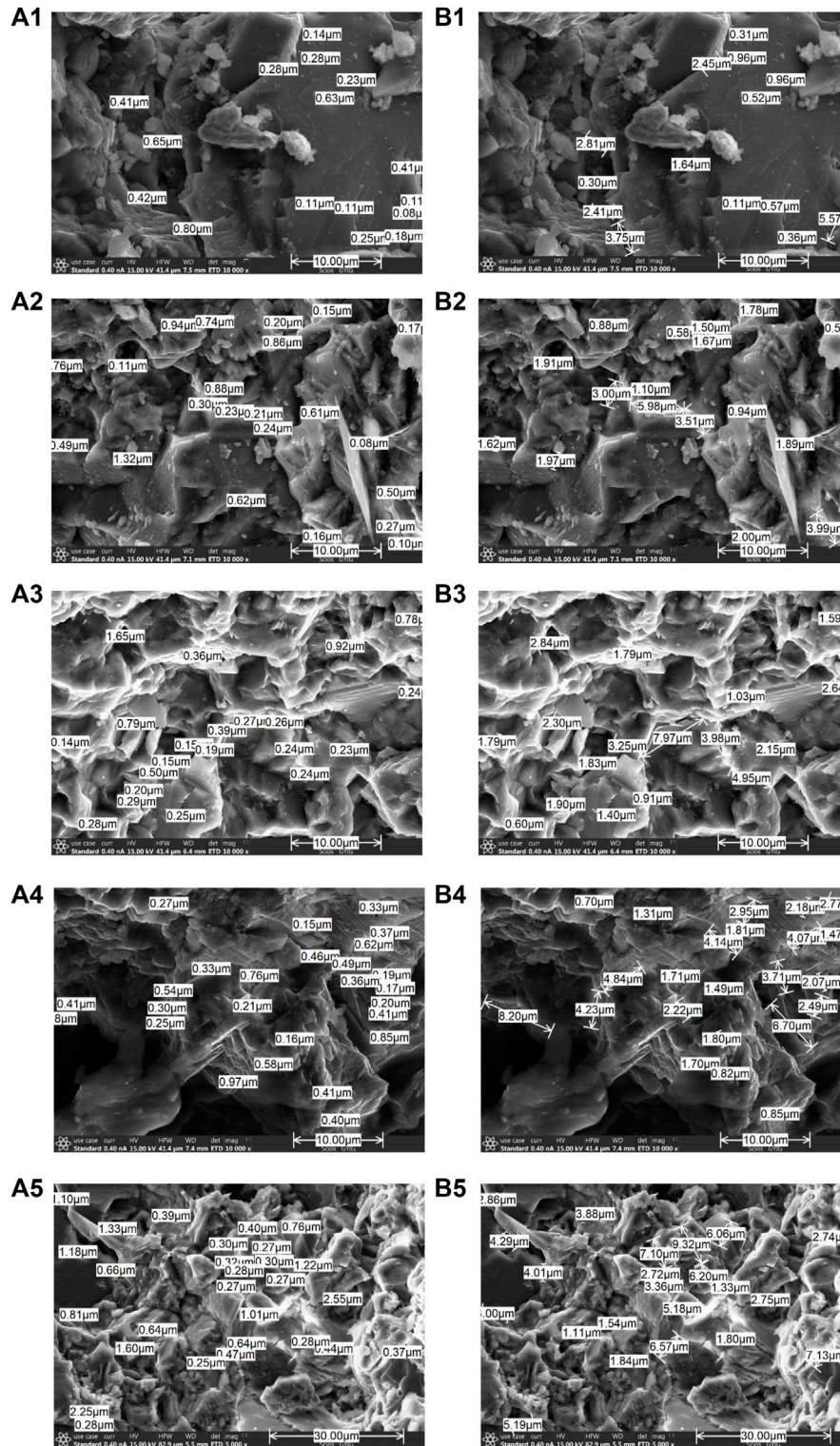
FIGURE 5 | Microstructure of jointed limestone with different water saturation times. **(A1–A5)**: Crack width of limestone samples dried and saturated for 1, 3, 5 and 7 days. **(B1–B5)**: Crack length of limestone samples dried and saturated for 1, 3, 5 and 7 days.

differences in the main ranges of microscopic pores width and length of the limestone samples with different water saturation times. The width of pores and cracks in dry samples is mainly concentrat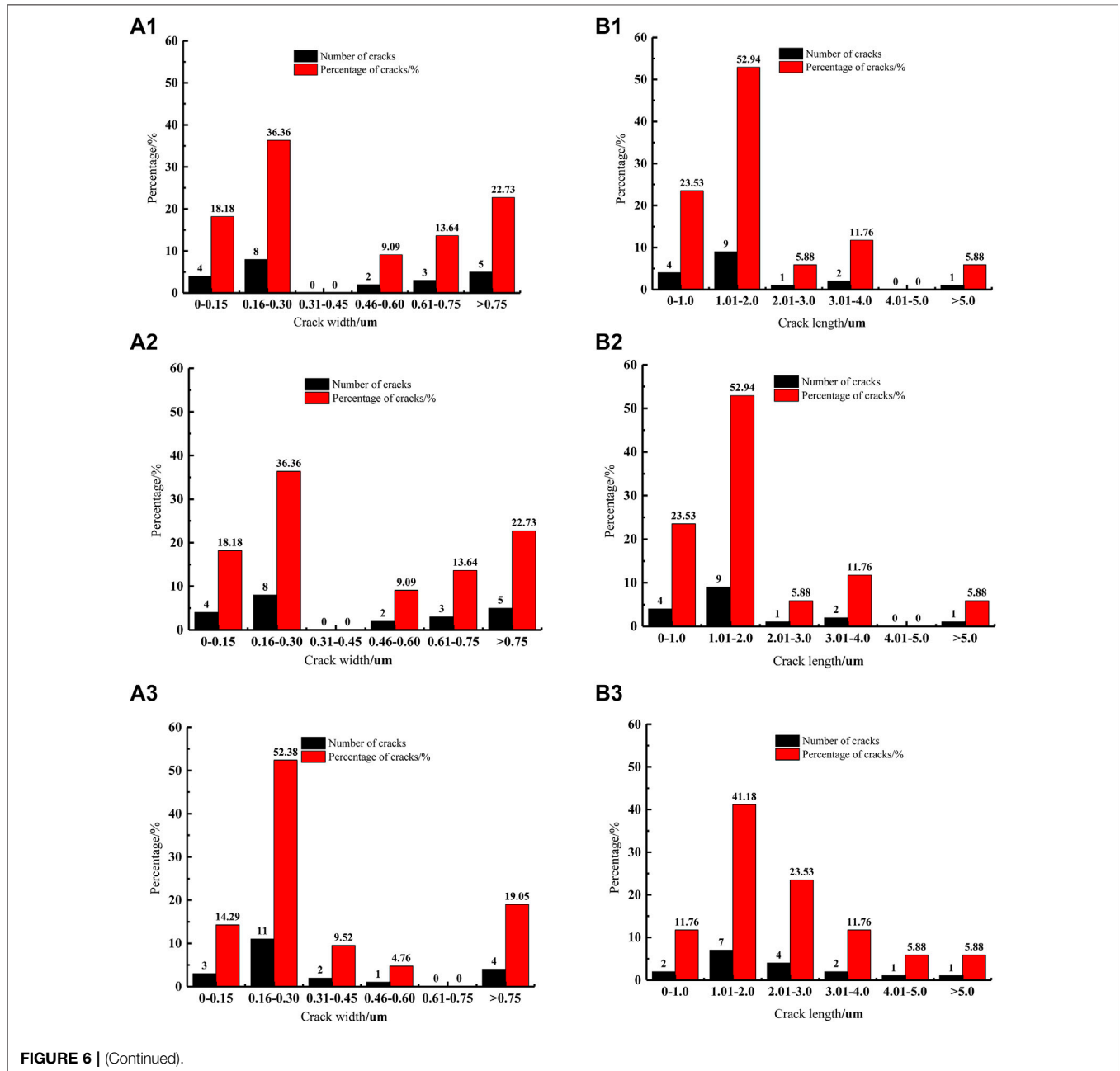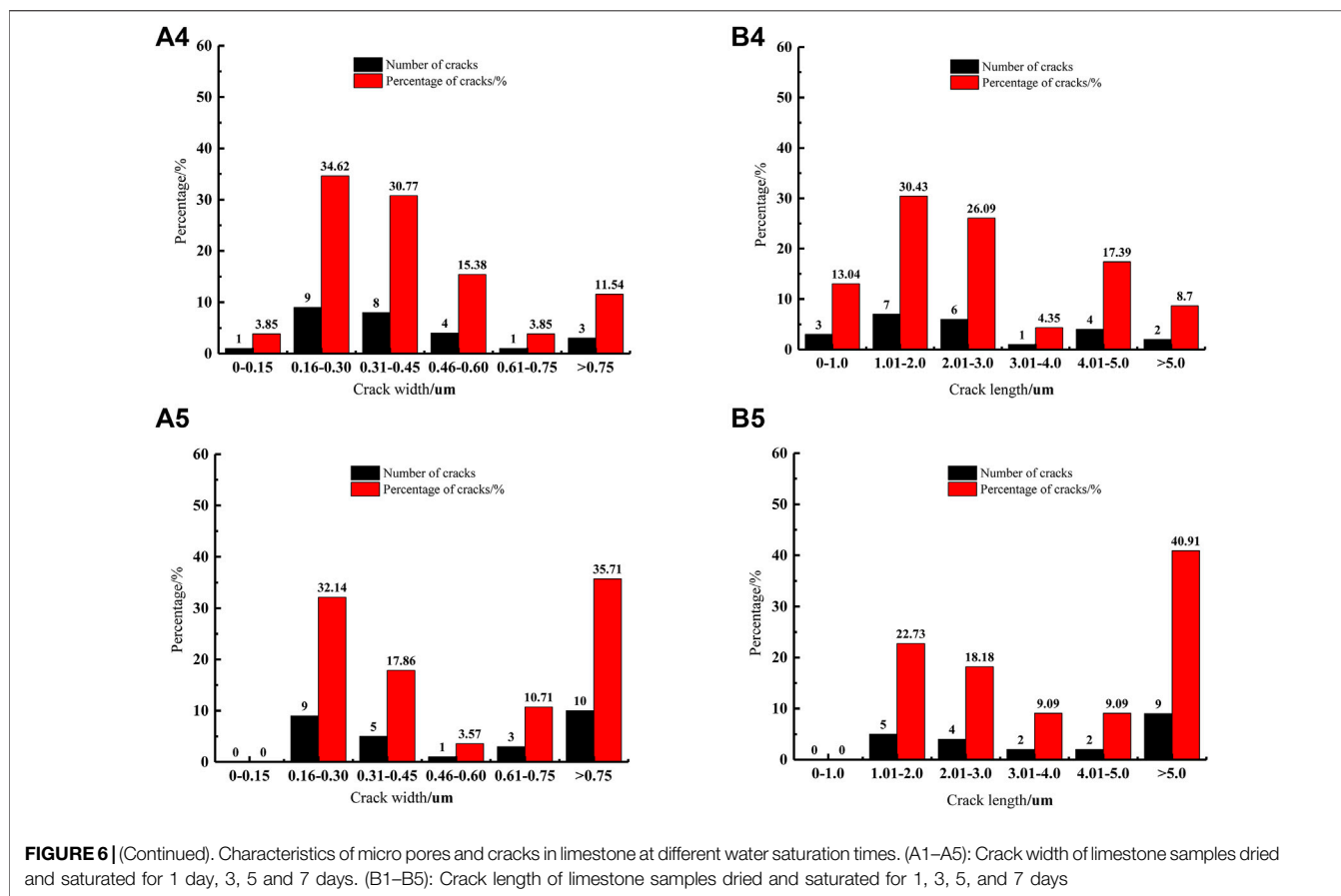ed in 0 ∼ 0.30 μm, and the number of cracks measured accounts for 60% of the total number of cracks. And the width of pores and cracks is mainly concentrated in

TABLE 3 | Characteristics of limestone pores and fissures at different water saturation times.

Water saturation time	Length of pores and fissures/um		Width of pores and fissures/um	
	Average value	Standard deviation	Average value	Standard deviation
Dry	1.62	1.60	0.32	0.22
1 Day	2.05	1.39	0.45	0.34
3 Days	2.52	1.79	0.41	0.36
5 Days	2.79	1.89	0.40	0.22
7 days	4.23	2.25	0.74	0.61

FIGURE 6 | (Continued).

FIGURE 6 | (Continued). Characteristics of micro pores and cracks in limestone at different water saturation times. (A1–A5): Crack width of limestone samples dried and saturated for 1 day, 3, 5 and 7 days. (B1–B5): Crack length of limestone samples dried and saturated for 1, 3, 5, and 7 days
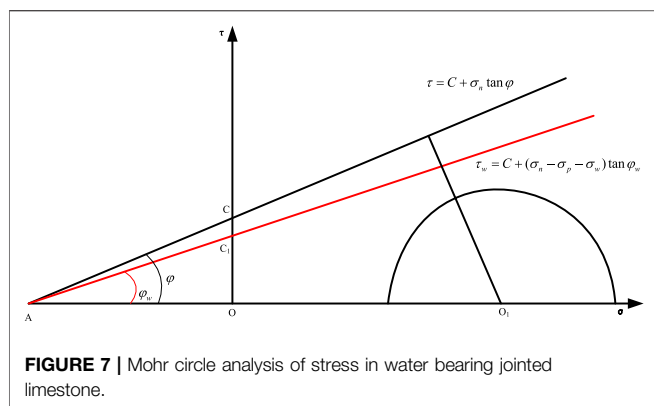
0 ~ 1.00 μm, and the number of cracks measured accounts for 57.14% of the total number of cracks. The width of pores and cracks in the sample after being saturated for 1 day is mainly concentrated in 0.16 ~ 0.30 μm and greater than 0.75 μm, and the number of cracks measured accounts for 59.09% of the total number of cracks. And the width of pores and cracks is mainly concentrated in 0 ~ 2.00 μm, the number of cracks measured accounted for 53.53% of the total number of cracks. The width of pores and cracks in the samples saturated with water for 3 days is mainly concentrated in 0.16 ~ 0.30 μm, and the number of cracks measured accounts for 52.38% of the total number of cracks. The width of pores and cracks in the sample after 5 days of water saturation is mainly concentrated in 0.16 ~ 0.45 μm, and the number of cracks measured accounts for 65.39% of the total number of cracks. The width of pores and cracks in the samples saturated with water for 7 days is mainly concentrated in 0.16 ~ 0.30 μm and greater than 0.75 μm, and the number of cracks measured accounts for 67.85% of the total number of cracks. And the width of pores and cracks is mainly concentrated in 1.00 ~ 2.00 μm and greater than 5.0 μm, the number of cracks measured accounts for 63.64% of the total number of cracks. Based on the above analysis, it can be found that with the gradual increase of the water saturation time, the main concentration range of the width and length of the pores and fractures gradually increases, indicating that water

saturation time has a promoting effect on the development of microscopic pores and fractures in limestone.

WEAKENING MECHANISM OF MECHANICAL PROPERTIES OF WATER BEARING JOINTED LIMESTONE

In the process of water saturation, the jointed limestone undergoes water-rock interaction. In the process of water-rock interaction, water mainly degrades the mechanical properties of jointed limestone from two aspects. First of all, after the jointed limestone is saturated with water, the original pores and fissures will be filled with water. The water in the pores and fissures will gradually increase with time, and will physically and chemically react with nearby hydrophilic minerals to generate new joints and fissures. The clay minerals will expand, resulting in an internal expansion force σ_p. Secondly, after the jointed limestone is saturated with water, lubrication is produced during uniaxial compression, reducing the internal friction angle inside the rock. After water saturation, the internal friction angle can be reduced by 6%~28% (Barton. 1973; Erguler and Ulusay, 2009; Alejano et al., 2012; Vilarrasa et al., 2019; Zhao, 2021). According to the Mohr-Coulomb theory (Yang et al., 2019; Zhao et al., 2020), in the process of water saturation of jointed limestone, the internal friction angle in **Eq. 3** will decrease and become φ_w, and the

FIGURE 7 | Mohr circle analysis of stress in water bearing jointed limestone.

FIGURE 8 | Failure modes of jointed limestone at different water saturation times. **(A)** Dry. **(B)** 1 day. **(C)** 3 days. **(D)** 5 days. **(E)** 7 days.

normal stress on the shear plane will be affected by the expansion forces σ_p and σ_w. After the jointed limestone is saturated with water, the modified Mohr-Coulomb formula is shown in **Eq. 4**. When the stress Mohr circle analysis (as shown in **Figure 7**) is applied, it can be found that after the jointed limestone is saturated with water, the stress Mohr circle is more likely to reach the limit equilibrium state, and the compressive strength of the jointed limestone will decrease.

$$\tau = C + \sigma_n \tan\varphi \tag{3}$$

Where τ is the shear stress, C is the cohesion, σ_n is the normal stress, and φ is the internal friction angle.

$$\tau_w = C + \left(\sigma_n + \sigma_p - \sigma_w\right)\tan\varphi_w \tag{4}$$

Where τ_w is the corrected shear stress, σ_p is the expansion force, σ_w is the pore water pressure, and φ_w is the internal friction angle after water saturation.

EFFECT OF WATER SATURATION TIME ON THE MACROSCOPIC FAILURE CHARACTERISTICS OF JOINTED LIMESTONE

To understand the influence of water saturation time on the macroscopic failure characteristics of jointed limestone, the macroscopic characteristics of jointed limestone with different water saturation times were analyzed. **Figure 8** shows that the macroscopic characteristics of the jointed limestone saturated for 0, 1, 3, 5 and 7 days. As indicated in the figure, the water saturation time has a certain influence on the macroscopic failure characteristics of the jointed limestone. The destruction levels of the samples saturated with water for 0 day is obviously higher than those of the samples saturated with water for 1, 3, 5, and 7 days. The integrity of the failure surface is worse, and the failure degree tends to decrease gradually with the increase of the water saturation time. The failure of jointed limestone is dominated by tension and shear failure. The failure of the sample basically starts from the vicinity of the joint, gathers and penetrates, and there is a certain number of secondary cracks
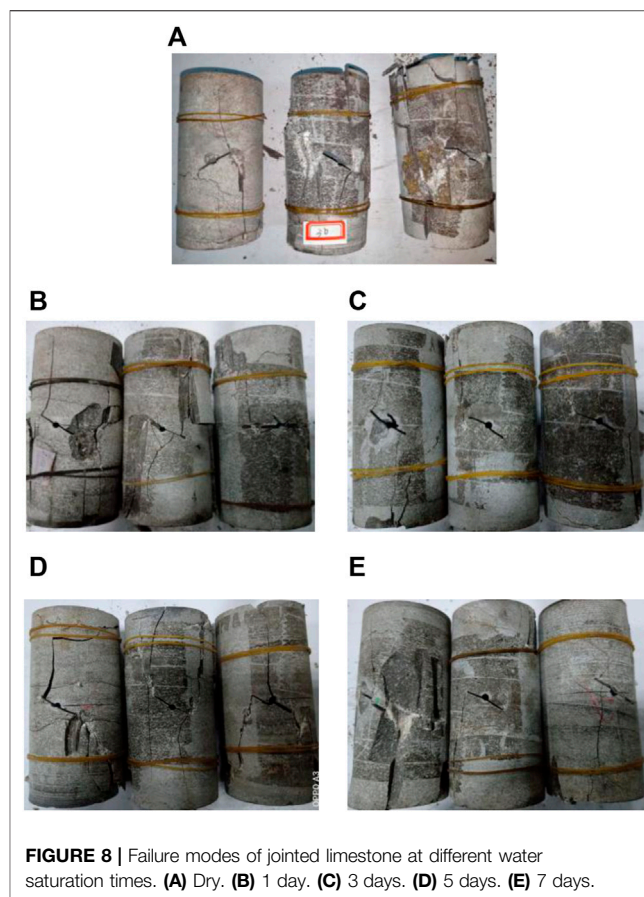
near it. However, with the increase of the water saturation time, the crack propagation tends to weaken.

CONCLUSION

To reveal the influence of water saturation time on the mechanical properties of jointed limestone, the stress-strain curve, compressive strength and elastic modulus of the limestone from northwest Guizhou are studied. After analysis and discussion, the main conclusions are drawn as follows:

(1) The water saturation time has an influence on the stress-strain curve of the jointed limestone. With the gradual increase of the water saturation time, the stress-strain curve changes significantly. The initial compaction period becomes significantly longer, the slope of the curve in the linear elastic stage gradually decreases, and there is a step rise or fall near the peak stress.

(2) There is a negative correlation between the peak compressive strength and elastic modulus of the jointed limestone and the water saturation time. The peak compressive strength and elastic modulus of the jointed limestone gradually decreases with the increase of the water saturation time.

(3) With the increase of the water saturation time, the skeleton particles of limestone samples are fractured and cracks

appear, and the length of microscopic pores and cracks gradually increases. The number and length of cracks are positively correlated with the water saturation time. In addition, the main concentration range of the microscopic pore and fracture length of limestone gradually increases. The phenomenon that the number of cracks and the length of cracks increase with the increase of the water saturation time is one of the reasons for the deterioration of the mechanical properties of the jointed limestone.

(4) In the process of water-rock interaction of jointed limestone, water mainly destroys the mechanical properties of jointed limestone from three aspects: physical and chemical reactions, lubrication, and formation of certain pore water pressure. Therefore, after the jointed limestone is saturated with water, the stress molar circle is more likely to reach the limit equilibrium state, and the compressive strength of the jointed limestone will decrease.

(5) When the jointed limestone samples are damaged, they basically start to crack from the vicinity of the joints, gather and penetrate, and a certain number of cracks will appear in the vicinity. The main failures are tension and tension shear, the degree of fracture is lower during failure, and the integrity of the failure surface is higher after failure.

DATA AVAILABILITY STATEMENT

AUTHOR CONTRIBUTIONS

HL, JW, and GX conducted experiments and collected experimental data; the full text was co-authored by HL and JW. XW is responsible for the data analysis and graphics rendering in **Section 3**. WL is responsible for the data analysis and graphics drawing in **Section 4**; YK is responsible for the editing of the article.

FUNDING

REFERENCES

Alejano, L. R., González, J., and Muralha, J. (2012). Comparison of Different Techniques of Tilt Testing and Basic Friction Angle Variability Assessment. *Rock Mech. Rock Eng.* 45, 1023–1035. doi:10.1007/s00603-012-0265-7

Barton, N. (1973). Review of a New Shear-Strength Criterion for Rock Joints. *Eng. Geol.* 7 (4), 287–332. doi:10.1016/0013-7952(73)90013-6

Coal Industry Ministry of the Peoples Republic of China (1988). *Measuring Methods of Physics-Mechanic Property for Coal and Rock*. Beijing: Criterion Press of China, 32–33.

Deng, H. F., Fang, J. C., and Li, J. L. (2017a). Mechanical Properties of Red-Bed Soft Rock on Saturated State. *J. China Coal Soc.* 42 (8), 1994–2002. doi:10.13225/j.cnki.jccs.2016.1735

Deng, H. F., Zhang, Y. C., and Li, J. L. (2017b). Effect of Moisture Content on Splitting Tensile Strength of Layered Sandstone. *Chin. J. Rock Mech. Eng.* 36 (11), 2778–2787. doi:10.13722/j.cnki.jrme.2017.1175

Duan, T. Z., and Ren, Y. P. (2019). Study on Uniaxial Compression Mechanical Properties of Sandstone with Different Moisture Content and Wave Velocity Method. *Coal Geol. Explor.* 47 (4), 153–158. doi:10.3969/j.issn.1001-1986.2019.04.023

Erguler, Z. A., and Ulusay, R. (2009). Water-Induced Variations in Mechanical Properties of Clay-Bearing Rocks. *Int. J. Rock Mech. Min. Sci.* 46 (2), 355–370. doi:10.1016/j.ijrmms.2008.07.002

Fan, C., Li, H., Qin, Q., He, S., and Zhong, C. (2020). Geological Conditions and Exploration Potential of Shale Gas Reservoir in Wufeng and Longmaxi Formation of Southeastern Sichuan Basin, China. *J. Petroleum Sci. Eng.* 191, 107138. doi:10.1016/j.petrol.2020.107138

Huang, W., Xiao, W. M., and Tian, M. T. (2020). Model Test Research on the Mechanical Properties of Irregular Columnar Jointed Rock Masses. *Rock Soil Mech.* 41 (7), 2349–2359. doi:10.16285/j.rsm.2019.1493

Li, T., Zhao, J. J., and Xie, M. L. (2018). Experimental Study on the Effect of Slate Rock Mechanics Properties Degradation by the Saturation-Time. *Sci. Tech. Eng.* 18 (6), 217–222.

Li, H., Tang, H., Qin, Q., Zhou, J., Qin, Z., Fan, C., et al. (2019). Characteristics, Formation Periods and Genetic Mechanisms of Tectonic Fractures in the Tight Gas Sandstones Reservoir: A Case Study of Xujiahe Formation in YB Area,

Sichuan Basin, China. *J. Petroleum Sci. Eng.* 178, 723–735. doi:10.1016/j.petrol.2019.04.007

Li, B., Liu, J., and Liu, Z. P. (2020). The Unloading Mechanical Properties of Shale with Different Water Saturation. *Rock Soil Mech.* 41 (Suppl. 2), 1–11. doi:10.16285/j.rsm.2019.1837

Li, H., Qin, Q., Zhang, B., Ge, X., Hu, X., Fan, C., et al. (2020a). Tectonic Fracture Formation and Distribution in Ultradeep Marine Carbonate Gas Reservoirs: A Case Study of the Maokou Formation in the Jiulongshan Gas Field, Sichuan Basin, Southwest China. *Energy fuels.* 34 (11), 14132–14146. doi:10.1021/acs.energyfuels.0c03327

Li, H. G., Yang, Z. K., and Li, H. M. (2020). Mechanical Characteristics and Failure Mechanism of Siltstone with Different Joint Thickness. *Adv. Civ. Eng.* 2020, 3824538. doi:10.1155/2020/3824538

Li, H., Wei, L., and Li, H. M. (2020b). Analysis of the Influence of Coal Thickness on the Physical and Mechanical Characteristics of Coal and Rock Mass. *Min. Safe. Environ. Prot.* 47 (6), 48–53. doi:10.19835/j.issn.1008-4495

Li, J., Li, G. Y., and Peng, W. L. (2020). The Strength and Deformation Characteristics of Saturated Weathered Granite under Freezing and Thawing Conditions. *J. Glaciol. Geo.* 42 (2), 1–9. doi:10.7522/j.issn.1000-0240.2020.0011

Li, H. G., Li, H. M., and Gao, B. B. (2021). Study on Acoustic Emission Characteristics in the Process of Fracture of Coal-Rock Combination Body with Different Thickness of Coal. *J. Henan Polytech. Univ. Nat. Sci. Ed.* 40 (5), 30–37. doi:10.16186/j.cnki.1673-9787.2019120077

Li, H. (2022). Research Progress on Evaluation Methods and Factors Influencing Shale Brittleness: A Review. *Energy Rep.* 8, 4344–4358. doi:10.1016/j.egyr.2022.03.120

Liu, H. Y., Wang, X. S., and Zhang, L. M. (2016). A Dynamic Damage Constitutive Model for Rock Mass with Non-persistent Joints under Uniaxial Compression. *Chin. J. Geo. Eng.* 38 (3), 426–436. doi:10.11779/CJGE201603005

Meng, Q.-X., Wang, H.-L., Xu, W.-Y., and Chen, Y.-L. (2019). Numerical Homogenization Study on the Effects of Columnar Jointed Structure on the Mechanical Properties of Rock Mass. *Int. J. Rock Mech. Min. Sci.* 124, 104127. doi:10.1016/j.ijrmms.2019.104127

Niu, S.-j., Ge, S.-s., Yang, D.-f., Dang, Y.-h., Yu, J., and Zhang, S. (2018). Mechanical Properties and Energy Mechanism of Saturated Sandstones. *J. Cent. South Univ.* 25 (6), 1447–1463. doi:10.1007/s11771-018-3839-z

Su, C. D., Sun, Y. N., and Zhang, Z. H. (2017). On the Effect of Water-Saturated State on Failure Energy of Sandstone from Coal Seam Roof Subjected to Uniaxial Compression. *J. Exp. Mech.* 32 (2), 223–231. doi:10.7520/1001-4888-16-118

Vasarhelyi, B. (2005). Statistical Analysis of the Influence of Water Content on the Strength of the Miocene Limestone. *Rock Mech. Rock Engng.* 38 (1), 69–76. doi:10.1007/s00603-004-0034-3

Vilarrasa, V., Carrera, J., Olivella, S., Rutqvist, J., and Laloui, L. (2019). Induced Seismicity in Geologic Carbon Storage. *Solid Earth.* 10, 871–892. doi:10.5194/se-10-871-2019

Wang, W., Li, H. M., and Yuan, R. F. (2016). Micromechanics Analysis and Mechanical Characteristics of Water-Saturated Coal Samples under Coupled Static-Dynamic Loads. *J. China Coal Soc.* 41 (3), 611–617. doi:10.13225/j.cnki.jccs.2015.0558

Wang, W., Li, H. M., and Gu, H. L. (2017). Experimental Study of Strength Characteristics of Water-Saturated Coal Specimens under 3D Coupled Static-Dynamic Loadings. *Chin. J. Rock Mech. Eng.* 36 (10), 2406–2414. doi:10.13722/j.cnki.jrme.2017.0545

Wang, C., Liu, C. W., and Liu, D. F. (2019). Experimental Study on Volume Effect of Saturated Fractured Sandstone under Uniaxial Compression. *Chin. J. Undergr. Space Eng.* 15 (5), 1331–1340.

Wen, M., Chen, Z., and Xu, J. Y. (2017). Static-dynamic Split Tensile Tests and Micro Analysis on Red-Sandstone with Different Moisture Contents. *Chin. J. Undergr. Space Eng.* 13 (1), 86–92.

Xia, Y., Zhang, C., Zhou, H., Hou, J., Su, G., Gao, Y., et al. (2020). Mechanical Behavior of Structurally Reconstructed Irregular Columnar Jointed Rock Mass Using 3D Printing. *Eng. Geol.* 268, 105509. doi:10.1016/j.enggeo.2020.105509

Yang, H., Zhang, J. X., and Shan, R. L. (2018). Experimental Study on Mechanical Properties of Frozen Saturated Single Fractured Rock Mass. *Rock Soil Mech.* 39 (4), 1245–1255. doi:10.16285/j.rsm.2016.0989

Yang, W., Zhang, Q., Ranjith, P. G., Yu, R., Luo, G., Huang, C., et al. (2019). A Damage Mechanical Model Applied to Analysis of Mechanical Properties of Jointed Rock Masses. *Tunn. Undergr. Space Technol.* 84, 113–128. doi:10.1016/j.tust.2018.11.004

Yilmaz, I. (2010). Influence of Water Content on the Strength and Deformability of Gypsum. *Int. J. Rock Mech. Min. Sci.* 47 (2), 342–347. doi:10.1016/j.ijrmms.2009.09.002

Zhang, E. F., Yang, G. S., and Tang, L. Y. (2019). Study on Influence of Water Content to Damage and Degradation Laws of Argillaceous Siltstone. *Coal Sci. Tech.* 47 (2), 14–20. doi:10.13199/j.cnki.cst.2019.02.003

Zhao, Y., Wu, Y., Xu, Q., Jiang, L., Huang, W., Zhang, P., et al. (2020). Numerical Analysis of the Mechanical Behavior and Failure Mode of Jointed Rock under Uniaxial Tensile Loading. *Adv. Civ. Eng.* 2020, 1–13. doi:10.1155/2020/8811282

Zhao, Z. H. (2021). Study on Water-Rock Interaction Mechanisms and Mechanical Behaviors of Single Rock Fractures. *Chin. J. Rock Mech. Eng.* 40 (Suppl. 2), 3063–3073. doi:10.13722/j.cnki.jrme.2021.0553

Zheng, G. H., Xu, J. Y., and Wang, P. (2017). A Dynamic/Static Experiment Research on the Red-Sandstone Mechanical Property under Different Saturated Degree. *J. Air Force Eng. Uni. Na. Sci. Ed.* 18 (1), 99–104. doi:10.3969/j.issn.1009-3516.2017.01.017